AAEC/E418

AUSTRALIAN ATOMIC ENERGY COMMISSION
RESEARCH ESTABLISHMENT
LUCAS HEIGHTS

AN ANALYSIS OF POWER TRANSIENTS OBSERVED IN THE SPERT II D_2O MODERATED CLOSE PACKED CORE

by

J.W. CONNOLLY
B.V. HARRINGTON

September 1977

ISBN 0 642 59625 5

AUSTRALIAN ATOMIC ENERGY COMMISSION
RESEARCH ESTABLISHMENT
LUCAS HEIGHTS

AN ANALYSIS OF POWER TRANSIENTS OBSERVED IN THE SPERT II D_2O MODERATED CLOSE PACKED CORE

by

J.W. CONNOLLY
B.V. HARRINGTON

ABSTRACT

The power transient behaviour of the very under-moderated SPERT II core B18/68 is analysed. The experimental conditions included core pressurisation and forced coolant flow. Generally good agreement is obtained between measured and calculated data.

National Library of Australia card number and ISBN 0 642 59625 5

The following descriptors have been selected from the INIS Thesaurus to describe the subject content of this report for information retrieval purposes. For further details please refer to IAEA-INIS-12 (INIS: Manual for Indexing) and IAEA-INIS-13 (INIS: Thesaurus) published in Vienna by the International Atomic Energy Agency.

TRANSIENTS; SPERT-II REACTOR; NUCLEAR CORES; BOILING; HEAT TRANSFER; SHUTDOWN; COOLANTS; FLUID FLOW

CONTENTS

1. INTRODUCTION

The transient tests performed with the SPERT II D_2O moderated and cooled core B18/68 are of interest because of the inclusion of forced coolant flow and core pressurisation in the range of initial test conditions. In calculating these transients, the former requires correct modelling of forced convection heat transfer during the transient and the latter provides a good test of either suppressing boiling heat transfer or causing it to occur at higher temperatures than is the case for unpressurised tests.

The methods used by Clancy, Connolly & Harrington [1975,6] to compute power transients in SPERT I reactors were used in this report for all tests with no coolant flow. For those tests with forced coolant flow a simple model of heat transfer from the fuel plate to the coolant across a static film of coolant has been found to provide reasonable agreement with experimental power burst shapes obtained with coolant velocities in the range 0.12 to 4.3 ms^{-1}.

2. CORE DESCRIPTION

The SPERT II close packed core B18/68 has been described in some detail by Johnson *et al.* [1965]. Following SPERT I usage, the core title signifies a core of 68 fuel elements each containing 18 B-type fuel plates. The water channel between fuel plates was 2.4 mm wide, and with 7 grams of ^{235}U per fuel plate the deuterium/uranium ratio for the core was 335, thus placing it in the intermediate neutron spectrum category. Moderator expansion and voiding effects would therefore be expected to predominate in the self-shutdown mechanisms operating during power transients.

The reactor contained eight control rods, two in each quadrant of the core, and a centrally located transient rod. The core was surrounded by an aluminium flow skirt, 12.7 mm thick, and with an internal diameter of 1.07 m. This complete structure was mounted in a pressure vessel 4.9 m high and 2.5 m dia. Coolant entered the bottom end of the flow skirt through a 0.6 m dia. nozzle, flowed upwards through the core and then reversed direction to flow downwards through the radial reflector and left the pressure vessel through four nozzles in the bottom head. A cross-sectional view of the reactor vessel and core structure is shown in Figure 1.

3. CALCULATION OF CORE REACTIVITY FEEDBACK COEFFICIENTS

The approach adopted by Clancy, Connolly & Harrington [1975,6] for assessing the adequacy of calculations of core reactivity coefficients, namely comparison of measured static or quasi-static core properties with calculated ones was used in this work. This comparison showed that the simple calculational scheme found adequate for the SPERT I cores gave very poor agreement with core parameters measured in B18/68. The poor agreement was attributed to neglect of the large variations in neutron spectrum across the core when group collapsing the core cross section data. The computational scheme that was evolved to handle this proved to be complex; the details are given in Appendix A.

The major features of the method were the group collapsing of cross sections from twenty-two to four groups over spectra appropriate to regions of the reactor rather than over a simple cell spectrum, and the use of group and region dependent bucklings in the final X-Y representation of the reactor. Although the final comparison of calculated and measured reactor parameters was not entirely satisfactory, and the calculational scheme contained some rather arbitrary or intuitive features, it was not considered worthwhile to devote further effort to resolving the remaining discrepancies, which primarily affected parameters of lesser significance in determining transient responses.

3.1 Results of Calculations

The results of reactivity measurements given by Johnson *et al.* [1965] are in units of dollars. In Table 1, where experimental and calculated values are compared, the experimental results have been converted to an absolute reactivity scale on the assumption that \$1=0.0075 $\delta k/k$.

TABLE 1

COMPARISON OF MEASURED AND CALCULATED CORE PARAMETERS

Parameter	Experimental	Calculated
Reactor excess reactivity	0.045	0.052
Prompt neutron lifetime (μs)	480	600
Core average void coefficient ($\delta k/k$ $\%^{-1}$)	-2.1×10^{-5}	-2.3×10^{-5}
Peak/average thermal flux	2.5	2.4
Whole reactor temperature coefficient at 20°C ($\delta k/k$ $°C^{-1}$)	-6.0×10^{-5}	-2.5×10^{-5}

The most serious discrepancy in this table is found for the whole-reactor temperature coefficient. Figure 2 shows the temperature dependence of this parameter as given by McClure & Johnson [1964], and as computed by the methods given in Appendix A. Attempts to isolate the causes of this discrepancy were not successful; good agreement between both sets of data would exist if either the experimental values were meant to be expressed in Celsius rather than Fahrenheit temperature scales, as shown in Figure 2, or the calculated value of the reflector void coefficient is increased by a factor of about 2.5. Because calculated reactivity perturbations in the reflector are sensitive to the values of axial buckling used in this region, the second possibility is the more likely explanation for the discrepancy; the same possibility is favoured to explain the observed difference between the calculated and measured value of the prompt neutron lifetime which is almost wholly determined by the properties of the reflector.

Because reasonable agreement between experiment and calculation was obtained for the spatial variation of the void coefficient and its absolute value in the core, and this coefficient is the major component of the core reactivity feedback coefficient, no further attempt was made to improve the agreement between the experimental and calculated values of the whole reactor temperature coefficient of reactivity.

TABLE 2

ZONE REACTIVITY FEEDBACK COEFFICIENTS (x 10^5)

θ(°C)	Zone 1			Zone 2		
	1/k δk/δθ expansion	1/k δk/δθ temperature	1/k δk/δθ total	1/k δk/δθ expansion	1/k δk/δθ temperature	1/k δk/δθ total
20	-2.88	-1.33	-4.21	-1.00	-1.73	-2.73
40	-6.36	-1.33	-7.69	-2.20	-1.73	-3.93
60	-9.20	-1.33	-10.5	-3.18	-1.73	-4.92
80	-11.5	-1.33	-12.9	-3.98	-1.73	-5.72
150	-17.5	-1.33	-18.9	-6.06	-1.73	-7.80

Core-only reactivity feedback coefficients, arising from perturbations of moderator density and temperature, were computed for each fuel box in one quadrant of the core. Because of the pronounced flux gradient at the core/reflector interface (Figure 3), the core was divided into two radial zones as shown in Figure 4 to allow boiling processes in the

calculated transients to begin at different times in each zone. The calculated reactivity coefficients in each zone were then weighted by power factors to give the zone values of the reactivity feedback coefficient as a function of moderator temperature θ. These are shown in Table 2.

4. TRANSIENT ANALYSIS

The point reactor kinetics/one-dimensional heat transfer code ZAPP [Clancy 1977] was used to calculate a representative range of transients from the B18/68 test series. The experimental value of the prompt neutron lifetime was used in all calculations.

The test series may be divided conveniently into two groups on the basis of whether forced coolant flow was present or not. The methods adopted to calculate power transients in each group will be described separately in the following two sections. Common input data to both groups are the thermal properties of fuel alloy, cladding and D_2O coolant and the constants of the inhour equation, in which eleven delayed neutron groups were used.

4.1 Transient Analysis Without Forced Coolant Flow

Each radial core zone was represented by a single half cell made up of half the fuel alloy thickness (0.25 mm), the cladding thickness (0.508 mm) and one half of the coolant channel thickness (1.2 mm). Reflective boundary conditions were assumed at each end of this cell. Five nodes were used in both fuel alloy and cladding; the coolant was represented as eighteen regions, each containing five nodes. The first fourteen of these regions, adjacent to the cladding, were 0.03 mm wide and the remaining four, 0.19 mm wide.

Heat transfer in the cell was assumed to proceed by conduction until the temperature of a water region exceeded the initial sub-cooling divided by the zone power form factor, plus the initial coolant temperature. The thermal conductivity of the region was then made large in the calculation, resulting in the propagation of a temperature front into the coolant as successive regions switch to a high conductivity state. This simulation of boiling heat transfer has been more fully described by Clancy, Connolly & Harrington [1975].

The inner and outer radial zones contained 6×10^5 and 3.3×10^5 cells respectively, and from the calculations described in Appendix A it was found that the inner zone generated 52.6% of the core power with a form factor of 1.18, and the outer zone the remainder with a form factor

of 1.63. Because the power maximum in the outer zone occurred on the outer edge of a fuel element at the core reflector boundary, it was considered that this would produce boiling of the zone coolant too early in a transient if used in the calculations. Instead a form factor of 1.11 was used which was calculated from the ratio of the highest rated fuel element in the zone to the average zone power.

4.2 Transient Analysis With Forced Coolant Flow

For these calculations the core was divided into four axial zones as well as the two radial ones. At the top and bottom of the core were essentially infinite zones of D_2O, since the time scale of the transients was much less than the circuit time of the coolant. From the bottom D_2O zone, coolant was assumed to flow axially through the core zones into the top D_2O zone and then back to the bottom D_2O zone thus completing the flow loops shown schematically in Figure 5.

ZAPP computes the amount of heat transferred by conduction from the fuel plate to the water during one time step, then removes a proportion (determined by the flowrate) of zone i coolant into zone i+1 coolant, replacing it with an equal volume of zone i-1 coolant. Before recommencing the heat transfer calculation in the next time step, the heat content of the transferred coolant is assumed to be uniformly added to the coolant in the zone to which it has been transferred.

Although this model is physically reasonable, ZAPP has been written with the heat conduction equation describing heat transfer from fuel plate to coolant, which is incompatible with the mixing of the coolant enthalpy described in the previous paragraph. Instead of rewriting the code to include forced convection heat transfer correlations as a boundary condition at the cladding/coolant interface, we decided to attempt a simple model of heat transfer which would be compatible with the existing ZAPP coding and the concept of bulk coolant temperature used in the usual treatment of forced convection heat transfer.

To do this, the eighteen water regions of Section 4.1 were reduced to two; the first, adjacent to the fuel plate, remained 0.03 mm wide and retained the static conductivity of D_2O. The second region encompassed the remainder of the coolant channel and was given an arbitrarily high conductivity to force an almost flat temperature profile across the region. The single axial zone reactivity coefficients of Table 2 were then apportioned to the four axial zones in the same proportions given by McClure & Johnson [1964] for the axial distribution of the measured void coefficient.

5. RESULTS OF CALCULATIONS

Thirty power transients produced by step reactivity additions to the core and one ramp induced transient have been calculated and the results compared with the experimental data given by Johnson, *et al.* [1965]. Table 3 gives the values of calculated and experimental burst parameters peak power (P_{max}), energy release to the time of peak power (E_{tm}), maximum cladding temperature at the time of peak power (θ_{tm}) and the burst shape parameter $\alpha_o E_{tm}/P_{max}$ where α_o is the initial inverse reactor period.

5.1 Results for Transients Without Forced Coolant Flow

The first subgroup in this category is formed from those tests performed without core pressurisation and the data are brought together in section A (Table 3). The level of agreement between calculation and experiment is about the same as previously reported for the SPERT I cores by Clancy, Connolly & Harrington [1975,6], although runs 8 and 9 demonstrate poor agreement between experiment and calculation for values of $\alpha_o E_{tm}/P_{max}$. The sharper turn around of the calculated power burst cannot have been caused by the premature appearance of boiling heat transfer since for neither run are the trigger temperatures reached before peak power.

The second subgroup (sections B & C, Table 3) is comprised of no flow transients with the reactor vessel pressurised to 240 and 133 MPa respectively. These pressures were sufficient to prevent coolant boiling for all runs except 18 and 20. Again the calculated power bursts show a tendency to be sharper than the observations although there are not enough of them to strongly support such a view. If the effect does exist it is probably because the calculated reactivity feedback coefficients depend too strongly on temperature.

5.2 Results for Transients With Forced Coolant Flow

The SPERT II program explored the effect of flowrate on transient behaviour for two values of initial reactor period, approximately 280 ms and 100 ms. The first set of results is shown in section D (Table 3). Reasonable agreement between experiment and calculation is again demonstrated except for the temperatures for runs 29 and 30. For run 29 the tabular data given by Johnson, *et al.* [1965] differ from those shown in graphical form which give a value of 75°C for θ_{tm}. It appears likely that the tabular data for θ_{tm}, runs 29 and 30 have been transposed in the preparation of the table.

Figure 6 compares calculated and measured power shapes for runs 29, 30 and 32. The calculations adequately describe the disappearance of a true pulse shape as the flowrate increases. This makes the usual burst parameters at the time of a well defined power peak impossible to determine at high flowrates.

The second data set (section E, Table 3), is for the transients where the initial reactor period is shorter than the coolant transit time across the core, for all flowrate values used in the tests. The experimental results show a very weak dependence of the burst parameters on flowrate, except for runs 39 and 45 where the coolant transit time across the core (140 ms) approaches the value of the initial reactor period. Although the calculations show the same trend, there appears to be a step change in the calculated burst parameters between flowrates of 427 and 1027 mm s^{-1}. The reason for this has not been discovered.

Because the full power history of this group of transients shows considerable structure after the first power burst, the ability of the calculational method to reproduce the observed power behaviour should be assessed. Shown in Figure 7 are the experimental and calculated power histories for runs 21, 23, 25, 26, and 39. (The data are plotted with an arbitrary time of zero for each test as an aid to clarity.) The calculations reproduce the broad features of the power oscillations and the final runout power quite well.

Only one ramp test was performed in the series, and this was for a ramp reactivity input of 0.00217 $\delta k/k\ s^{-1}$ starting from a power of 10 kW and stopping when the reactivity input reached 0.0102 $\delta k/k$. The results of experiment and calculation are shown in section F (Table 3) and Figure 8.

All the calculations discussed above were performed with a fixed value of 0.03 mm for the thickness of the static layer of D_2O adjacent to the fuel plate. Some calculations were run with ZAPP to ascertain the effect of varying the thickness of this layer. Shown in Figure 9 are the results obtained for run 32. Although decreasing the layer thickness from 0.03 mm has little effect on the power trace, an increase produces power oscillation which becomes severe for a thickness of 0.12 mm. This may be a consequence of a greater time lag between energy released in the fuel plate, appearing in the bulk coolant.

TABLE 3

COMPARISON OF MEASURED AND CALCULATED BURST PARAMETERS

	Run No.	P_i MPa	V_i (mm s^{-1})	τ_o (ms)	α_o (s^{-1})	θ_i (^oC)	P_{max} (MW)		Expt. / Calc.
							Expt.	Calc.	
A	2	0	0	5100	0.196	22	1.4	1.2	1.17
	5	0	0	1770	0.56	22	4.0	3.6	1.11
	6	0	0	840	1.19	22	9.1	8.3	1.10
	7	0	0	610	1.63	22	11	13	0.87
	8	0	0	460	2.17	22	16	19	0.84
	9	0	0	227	4.40	22	42	59	0.71
	10	0	0	158	6.30	22	106	109	0.97
	11	0	0	110	9.07	22	189	197	0.96
	12	0	0	88	11.4	22	237	273	0.87
	13	0	0	74	13.5	22	287	358	0.80
	41	0	0	150	6.7	56	78	79	0.99
B	14	240	0	282	3.5	22	38	43	0.88
	15	240	0	182	5.5	22	79	96	0.82
	16	240	0	250	4.0	22	47	54	0.87
	17	240	0	157	6.4	21	97	127	0.76
	18	240	0	97	10.3	22	241	309	0.78
C	19	133	0	210	4.8	21	78	74	1.05
	20	133	0	100	10.0	22	267	284	0.94
	27	133	0	260	3.8	23	44	50	0.88
D	27	133	0	260	3.8	23	44	50	0.88
	29	133	731	280	3.6	26	40	45	0.90
	30	133	2134	270	3.7	26	65	82	0.79
	31	133	2591	290	3.4	27	88	~110	-
	32	133	3139	270	3.7	28	101	~120	-
E	20	133	100	10.0	10.0	22	267	284	0.94
	21	133	122	93	10.7	22	266	272	0.98
	23	133	427	91	11.0	22	265	299	0.89
	25	133	1067	91	11.0	24	257	335	0.77
	26	133	2134	100	10.0	27	263	330	0.80
	39	133	4267	105	9.5	40	248	341	0.73
	45	133	4267	98	10.2	55	223	333	0.67
F	60	133	2134	RAMP	0.00217 s^{-1}	33	116	150	0.77

TABLE 3 (Continued)

E_{tm} (MJ)		Expt./Calc.	θ_{tm} (°C)		Expt./Calc.	$\alpha_o E_{tm}/P_{max}$		Expt./Calc.
Expt.	Calc.		Expt.	Calc.		Expt.	Calc.	
-	13.3	-	44	36	1.22	-	2.26	-
16.8	14.7	1.14	57	50	1.15	2.35	2.28	1.03
17.8	14.9	1.19	74	62	1.19	2.32	2.14	1.08
14.6	15.7	0.93	84	71	1.20	2.16	2.03	1.06
17.1	17.0	1.01	95	82	1.15	2.32	1.93	1.20
21.0	21.8	0.96	105	95	1.11	2.20	1.62	1.36
25.5	26.3	0.97	122	119	1.02	1.51	1.51	1.00
28.9	31.3	0.92	133	132	1.01	1.39	1.44	0.97
30.2	36.0	0.84	139	141	0.99	1.45	1.50	0.97
31.2	40.8	0.76	147	159	0.92	1.47	1.53	0.96
18.1	18.5	0.98	79	65	1.21	1.59	1.57	1.01
21.9	22.5	0.97	131	120	1.09	2.01	1.82	1.10
30.0	31.6	0.95	208	182	1.14	2.08	1.81	1.15
23.6	24.3	0.97	144	133	1.08	2.01	1.81	1.12
29.7	35.7	0.83	212	210	1.01	1.96	1.80	1.09
40.0	48.8	0.82	228	256	0.89	1.71	1.63	1.05
29.1	27.7	1.05	168	156	1.08	1.79	1.81	0.99
-	45.0	-	200	230	0.87	-	1.58	-
21.2	23.7	0.89	117	129	0.90	1.83	1.80	1.02
21.2	23.7	0.89	117	129	0.90	1.83	1.80	1.02
22.3	26.1	0.85	104	69	1.51	2.01	2.09	0.96
47.5	52.2	0.91	74	109	0.68	2.7	2.35	1.17
-	~163	-	-	159		-	-	-
-	~144	-	-	149		-	-	-
-	45.0	-	200	230	0.87	-	1.58	-
41.0	47.2	0.86	198	202	0.98	1.64	1.85	0.89
41.5	45.7	0.91	198	205	0.96	1.72	1.68	1.02
42.2	54.3	0.78	186	237	0.78	1.81	1.78	1.02
46.1	59.4	0.78	193	230	0.84	1.75	1.80	0.97
54.8	69.3	0.79	180	244	0.73	2.09	1.93	1.08
47.1	63.6	0.74	155	153	1.01	2.15	1.95	1.10
-	44.6	-	197	142	1.39	-	-	-

6. CONCLUSIONS

The simple model of boiling heat transfer used in the transient analysis without forced coolant flow in the SPERT II core B18/68 has satisfactorily reproduced the experimental data for transients terminated with the cladding temperature above the saturation temperature of the coolant. Because of the dominance of the void coefficient in the total reactivity feedback coefficient for this core, this success further strengthens the conclusion reached by Clancy, Connolly & Harrington [1976] in their study of SPERT I cores that shutdown is achieved by boiling heat transfer without the development of large steam void fractions. The effect of suppressing or delaying boiling heat transfer by pressurising the core has been reproduced well by the calculations reported here.

The simple model which is incorporated in ZAPP has reproduced the detail of transients with a wide range of coolant flowrates quite adequately. Although the assumptions in the model of a static boundary layer and a layer of high conductivity bulk coolant appear rather arbitrary, the results of the calculations suggest that this very simple physical modelling of flowrate is enough to enable fast transients to be successfully calculated. A notable feature of the results is that the model does not depend on flowrate.

7. ACKNOWLEDGEMENT

The authors wish to thank B.E. Clancy for developing the coolant flow model used in ZAPP.

8. REFERENCES

Clancy, B.E. [1977] - ZAPP - A program for reactor power transient studies. AAEC/E report to be published.

Clancy, B.E., Connolly, J.W. & Harrington, B.V. [1975] - An analysis of power transients observed in SPERT I reactors. Part I: Transients in aluminium plate-type reactors initiated at ambient temperatures. AAEC/E345.

Clancy, B.E., Connolly, J.W. & Harrington, B.V. [1976] - An analysis of power transients observed in SPERT I reactors. Part II: Dependence of burst parameters on initial temperature and core moderation. AAEC/E383.

Johnson, R.L., Larson, H.A., McClure, J.A. & Norberg, J.A. [1965] - An analysis of the excursion behaviour of a highly enriched plate-type D_2O moderated core in SPERT II. IDO 17109.

McClure, J.A. & Johnson, R.L. [1964] - Critical loading and initial static experiments in the SPERT II reactor with a close packed D_2O moderated core. IDO 16996.

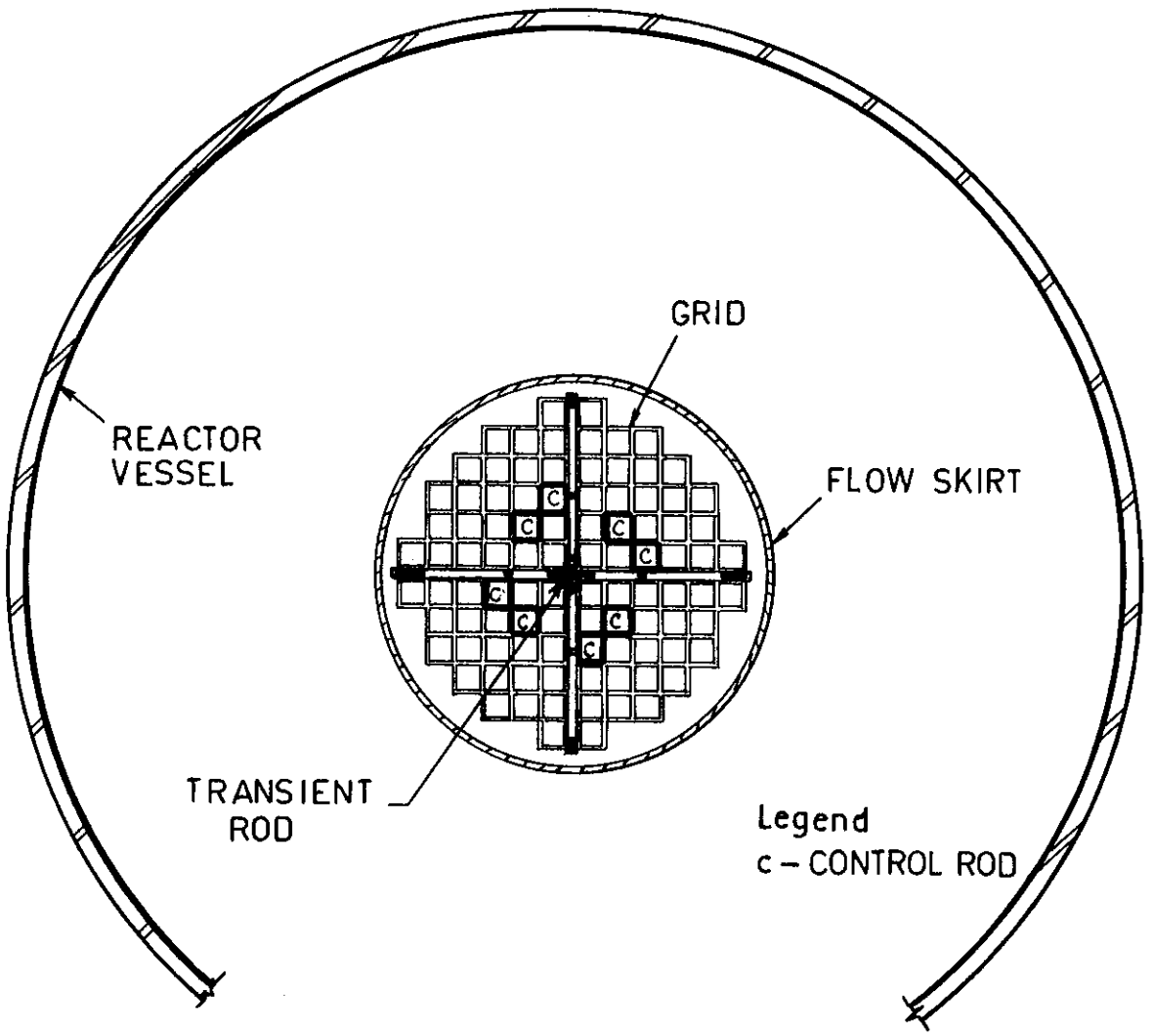

FIGURE 1. CROSS SECTION OF THE REACTOR VESSEL AND CORE STRUCTURE

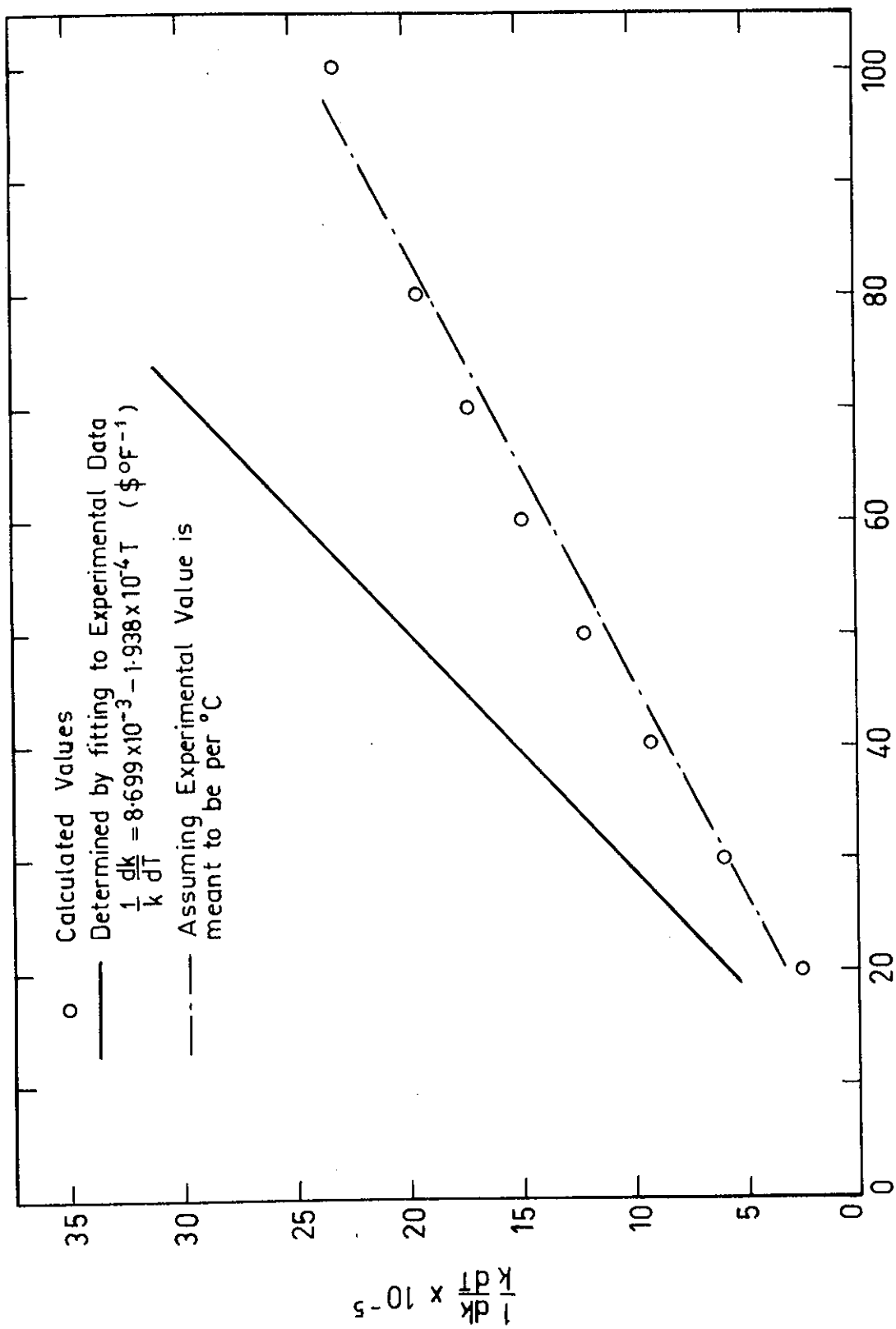

FIGURE 2. WHOLE REACTOR TEMPERATURE COEFFICIENT OF REACTIVITY

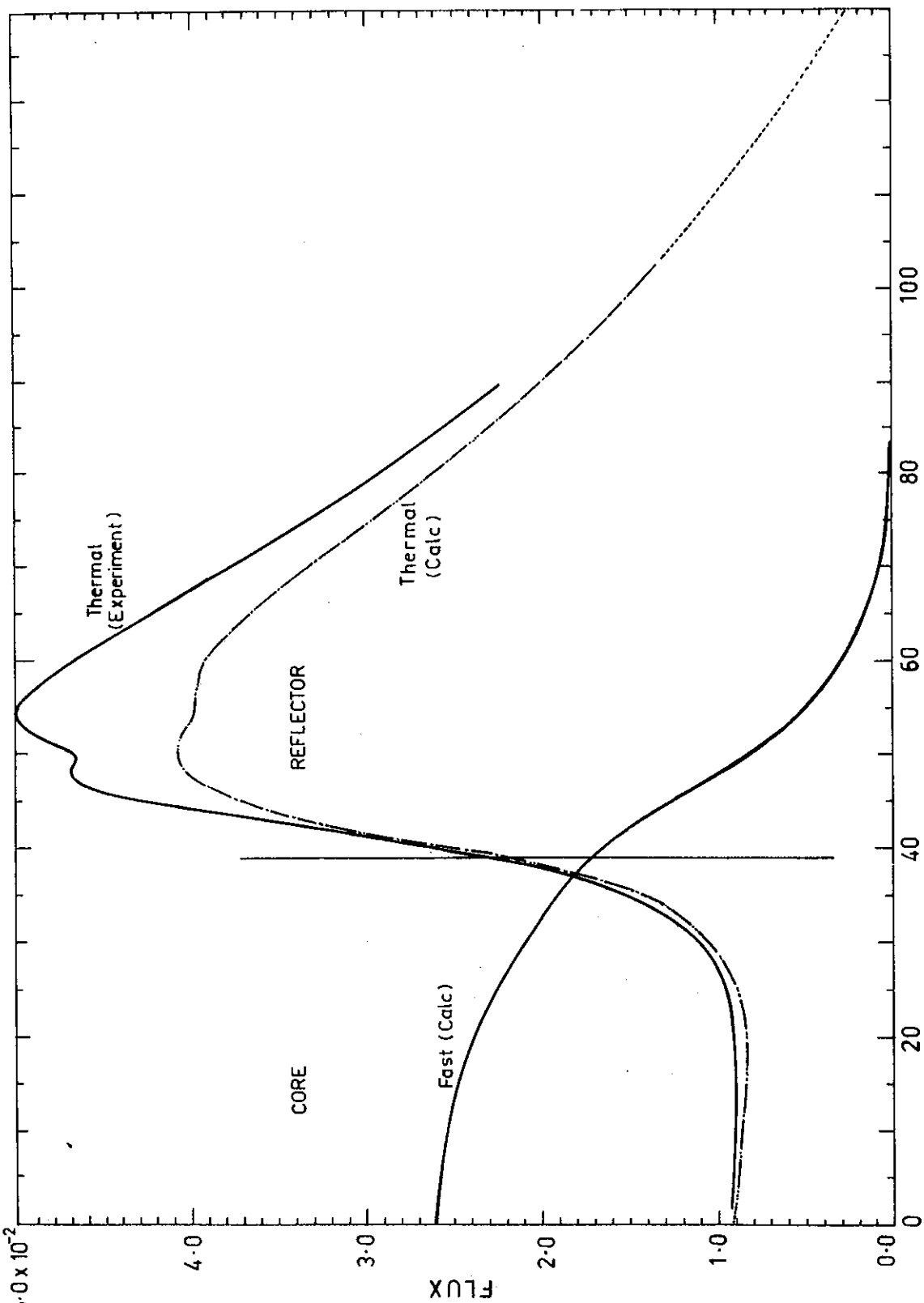

FIGURE 3. RADIAL FLUX DISTRIBUTIONS

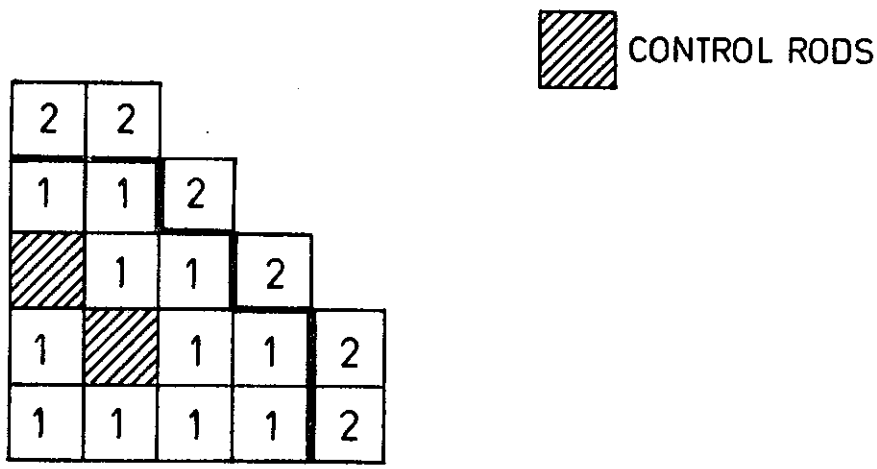

FIGURE 4. RADIAL SUB-DIVISION OF THE CORE

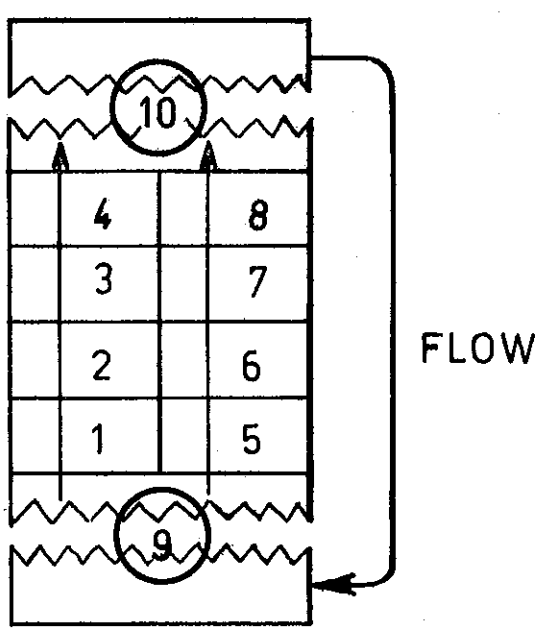

FIGURE 5. AXIAL SUB-DIVISION OF THE CORE FOR FLOW MODEL

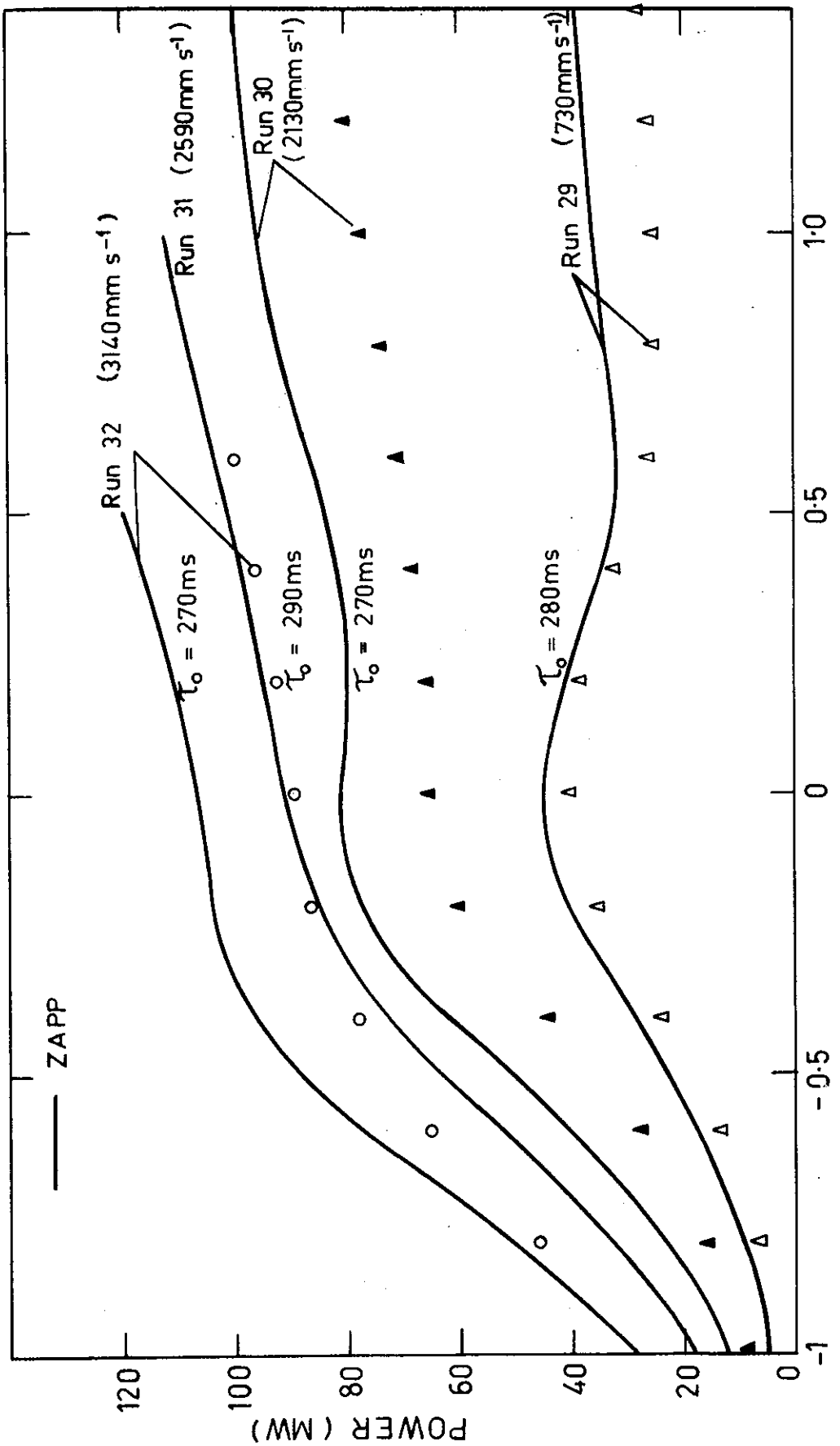

FIGURE 6. CALCULATED AND MEASURED POWER TRANSIENTS FOR RUNS 29, 30, 31 AND 32

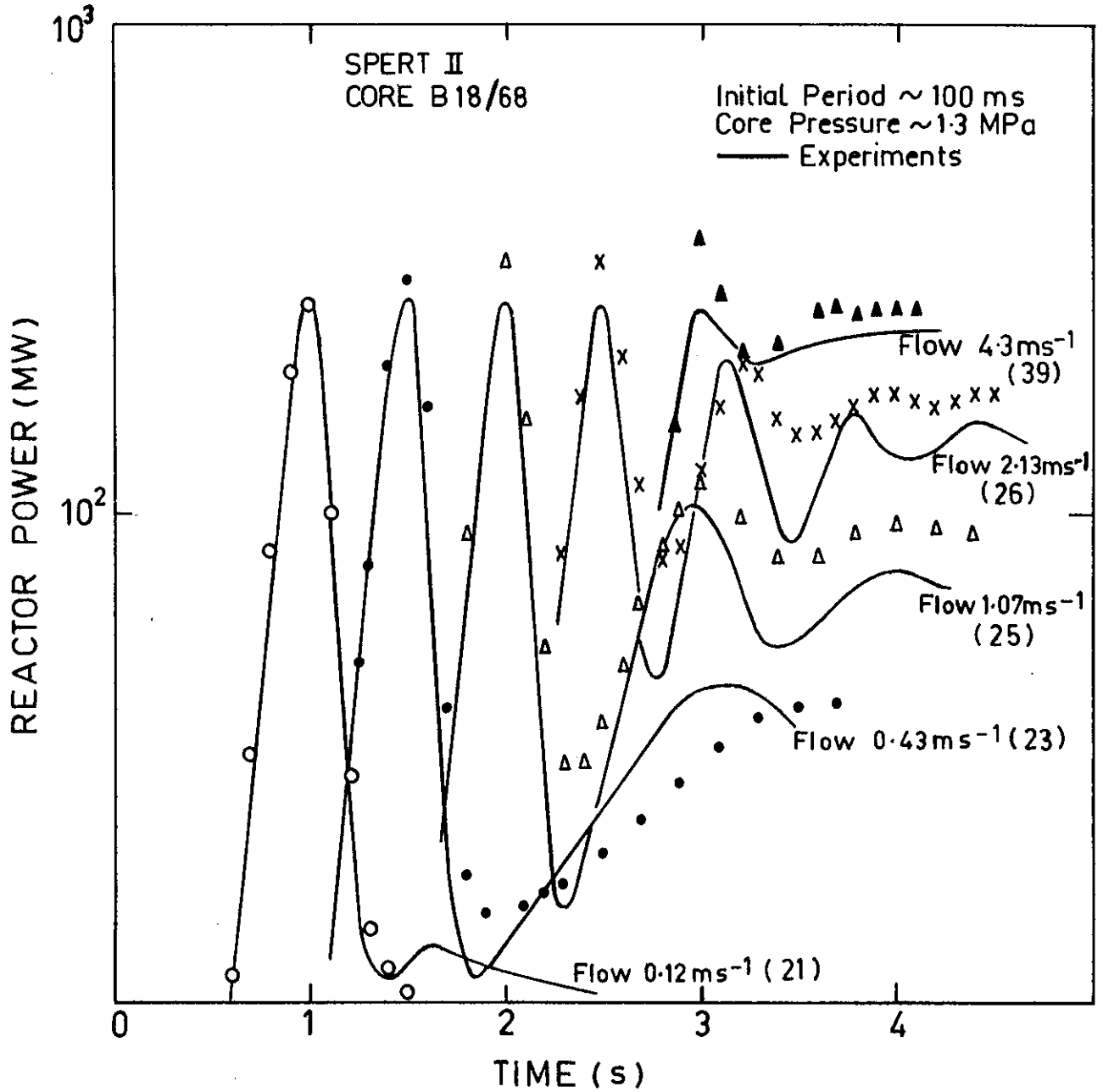

FIGURE 7. CALCULATED AND MEASURED POWER TRANSIENTS FOR RUNS 21, 23, 25, 26 AND 39

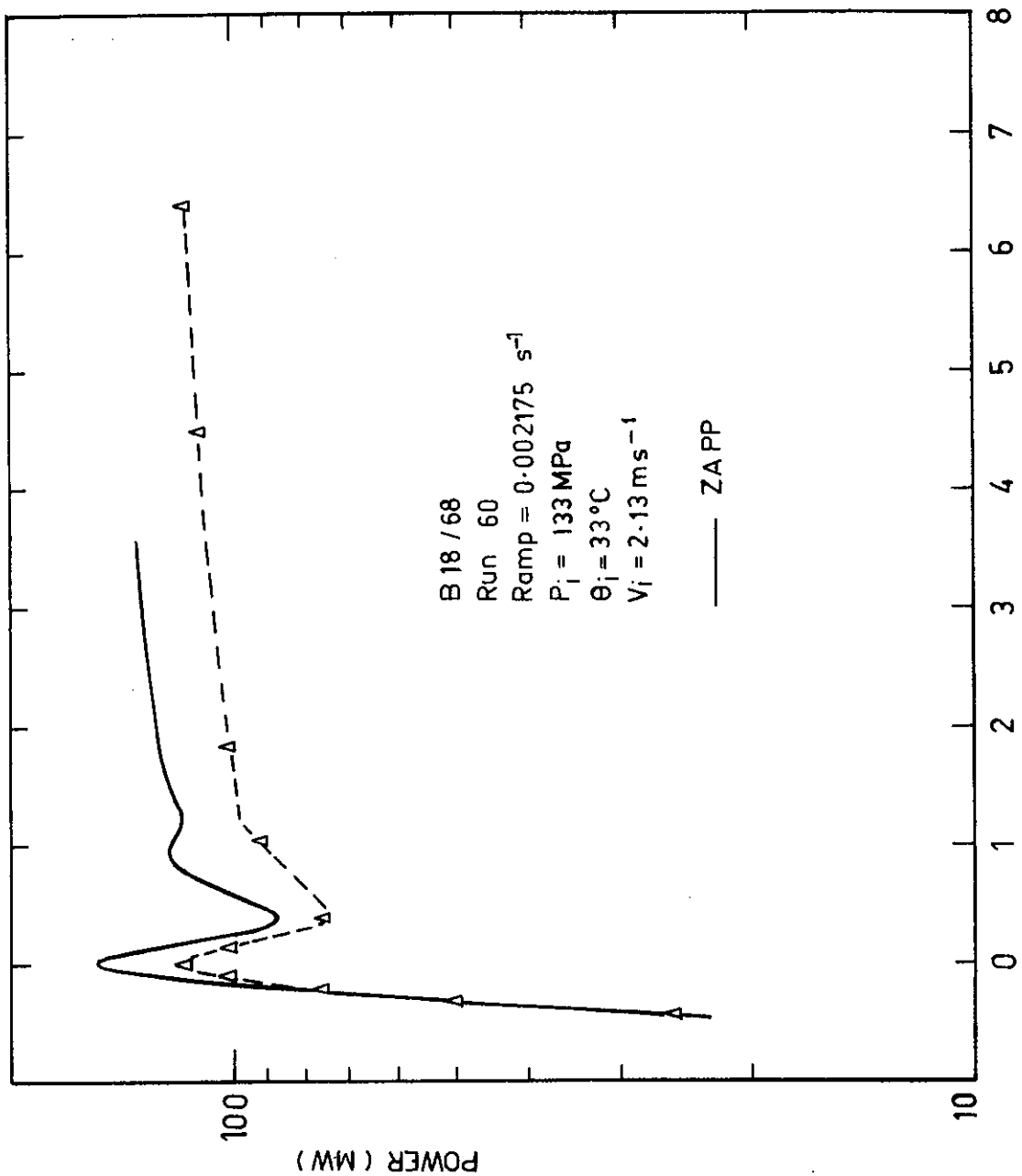

FIGURE 8. CALCULATED AND MEASURED POWER TRANSIENT FOR RUN 60

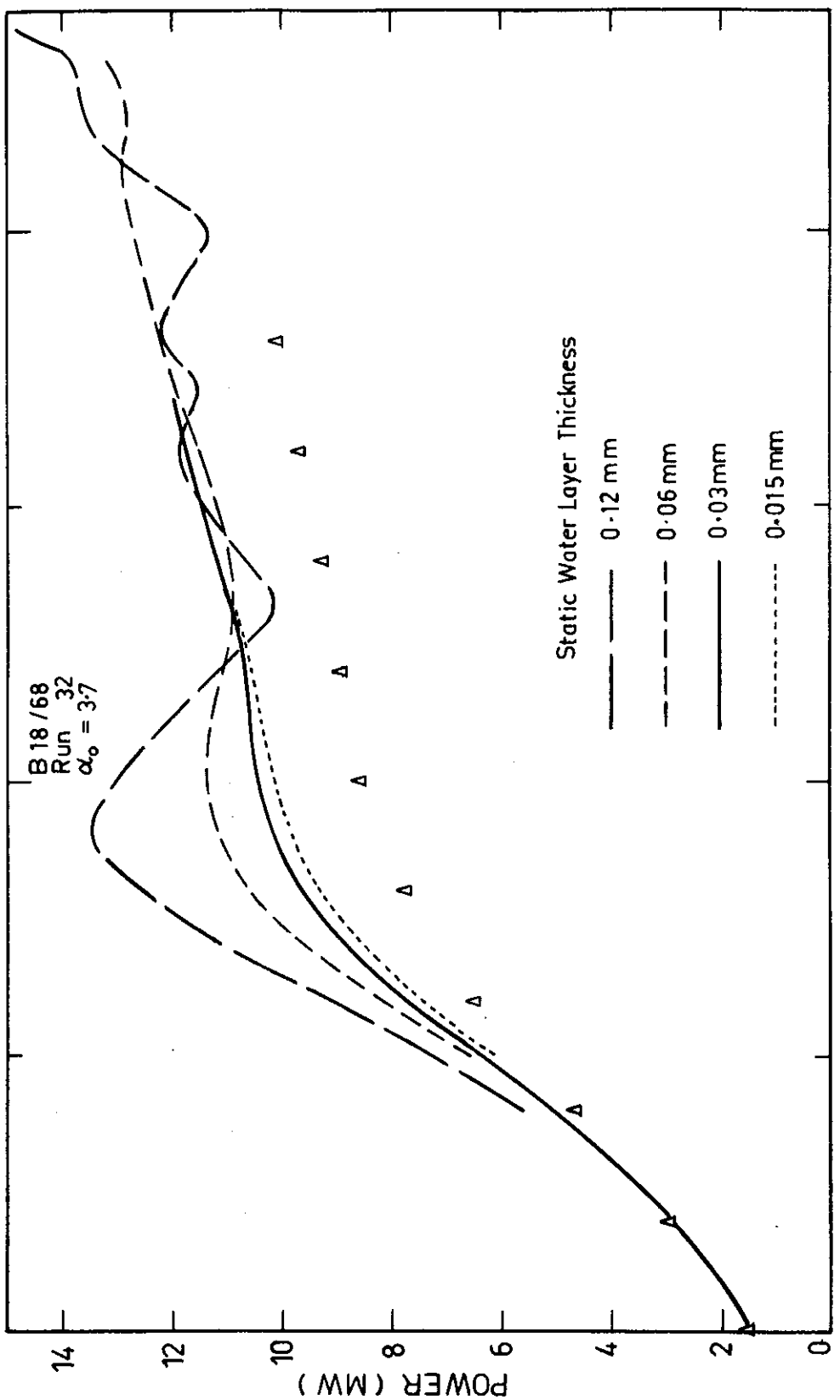

FIGURE 9. EFFECT OF BOUNDARY LAYER THICKNESS ON CALCULATED TRANSIENT FOR RUN 32

APPENDIX A

CALCULATION OF CORE PARAMETERS

(a) AUS Module MIRANDA

The data preparation code MIRANDA was used to prepare a 22-group cross section set for D_2O, Al and the fuel plates from the 128-group cross section data library AUS.ENDFB. The calculation included multi-region resonance treatment, a homogeneous flux solution and group condensation.

(b) AUS Module ICPP

The collision probability module ICPP, and cross sections generated in (a) were used to calculate 22-group fluxes within a cell representing an individual fuel plate and associated D_2O as shown in Figure A1. Reflective left and right boundary conditions were used.

(c) AUS Module EDIT1D

A buckling search was performed by the editing module EDIT1D to give critical fluxes for the cell in (b). These fluxes were used to smear the fuel plate and D_2O to give 22-group 'fuel region' cross sections.

(d) AUS Module ANAUSN

The one-dimensional S_n transport module ANAUSN (together with fuel region cross sections from (c) and D_2O and Al cross sections from (a)) was used to calculate 22-group fluxes in a fuel box (Figure A2). The volumes of 'fuel' and D_2O/Al in the one-dimensional representation of Figure A3 were preserved.

(e) AUS Module EDIT1D

A buckling search was done to give critical fluxes for the fuel boxes in (d). These were then used to smear the 'fuel' and D_2O/Al cross sections to give 22-group 'fuel box' cross sections.

(f) AUS Module POW

The diffusion code POW was used with 'fuel box' cross sections from (e) and D_2O and Al cross sections from (a) to calculate the 22-group reactor flux spectrum, assuming one-dimensional cylindrical geometry (Figure A4). This spectrum was used to collapse the 22-group cross section data to four groups. The D_2O data from (a) were treated as four different materials, D_2O, 1, 2, 3 and 4 and collapsed over the flux spectra in four annular regions of the radial reflector (Figure A5). Similarly, the 'fuel' cross sections were collapsed over two annular regions to give data for FUEL 1 and 2.

(g) AUS Module POW

The four-group cross sections from (f) were used in a cylindrical R-Z POW calculation of the reactor to determine region and energy dependent axial bucklings.

(h) AUS Module POW

The axial bucklings from (g) could have been used directly in the X-Y reactor model, but an attempt was made to improve the buckling data as follows. A one-dimensional cylindrical, four-group calculation with the axial bucklings from (g) was done with a search routine for a scaling factor for the axial bucklings that would make k_{eff} for the one-dimensional cylindrical calculation identical to that obtained from the R-Z calculation.

(i) AUS Module POW

The four-group cross sections for FUEL 1 and 2, and D_2O, 1, 2, 3 and 4 from (f), together with the region and energy dependent bucklings from (h) were used in the X-Y reactor calculation. Real and adjoint flux solutions were obtained, and a perturbation theory subroutine employed to calculate reactivity coefficients associated with temperature and density changes.

REFLECTIVE	0·1957 cm
D_2O	0·0762 cm
Al	0·0254 cm
Alloy	0·0
REFLECTIVE	

FIGURE A1. CELL CONSISTING OF AN INDIVIDUAL FUEL PLATE

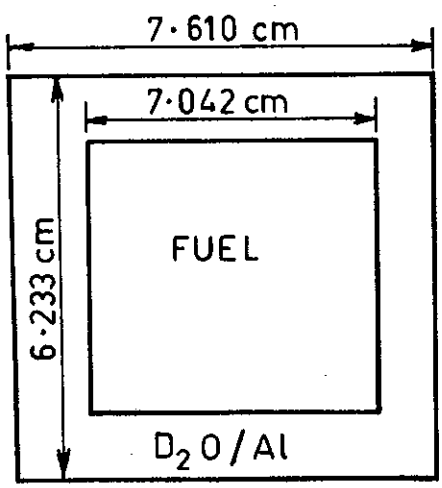

FIGURE A2. FUEL BOX CELL

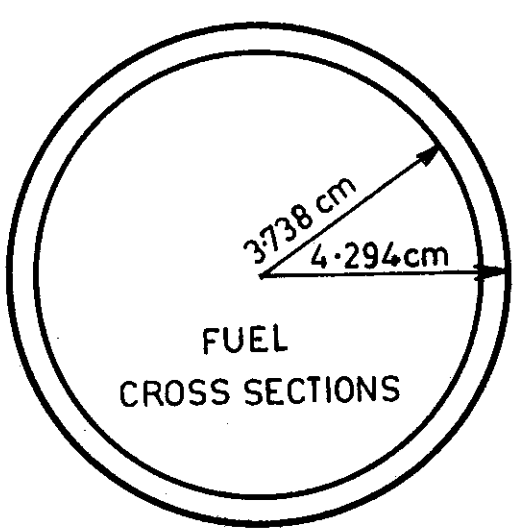

FIGURE A3. CYLINDRICAL REPRESENTATION OF A FUEL BOX

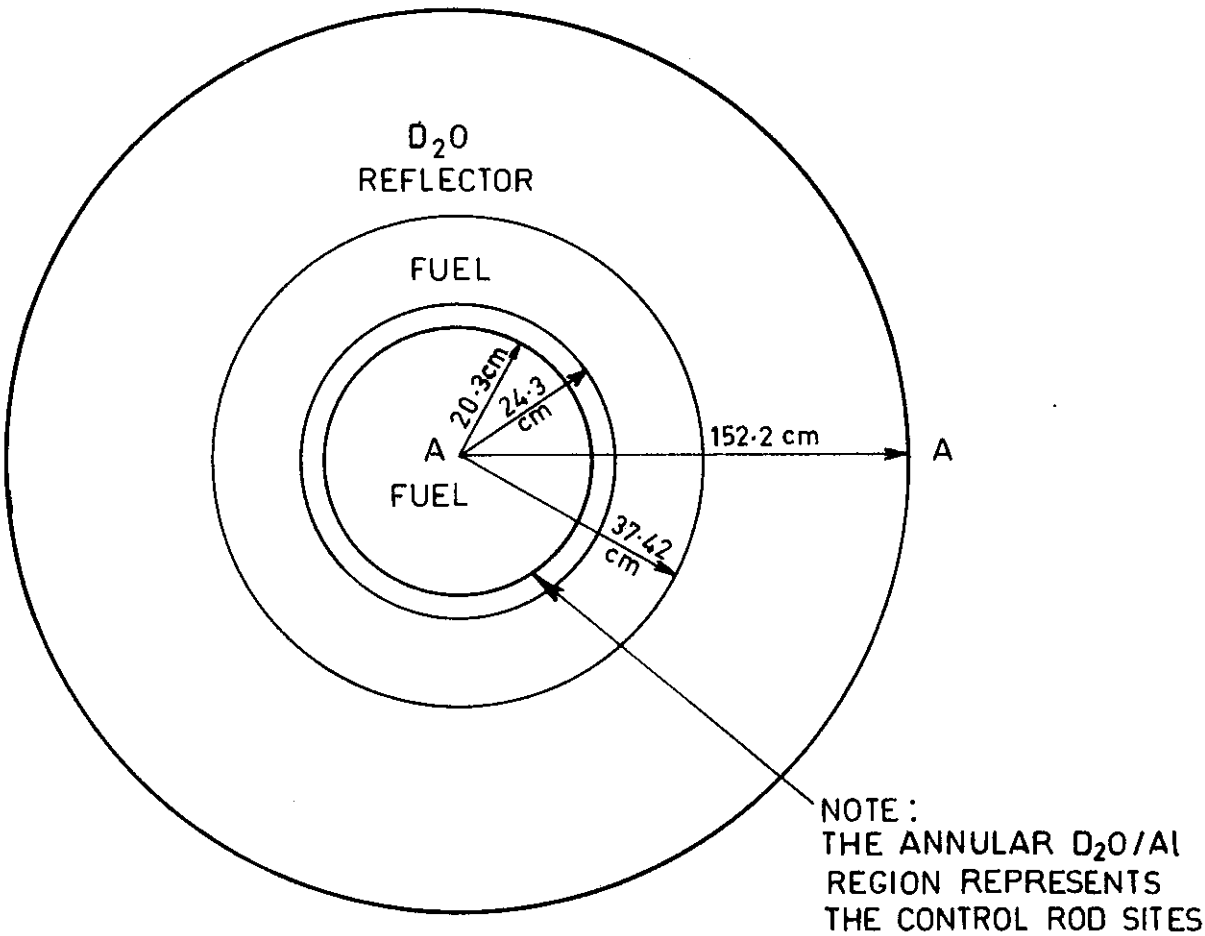

FIGURE A.4 1-D CYLINDRICAL REACTOR REPRESENTATION

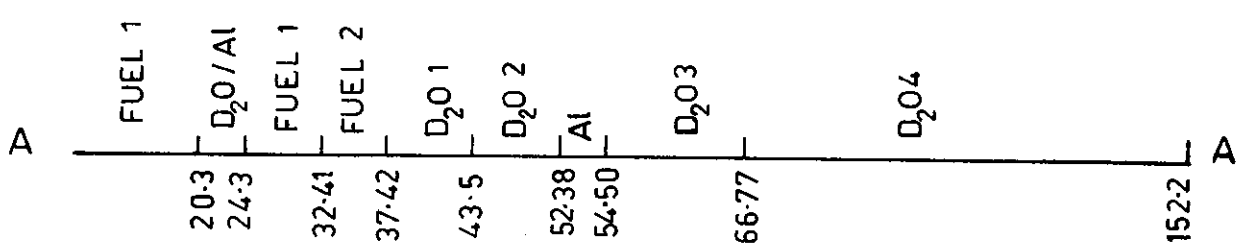

FIGURE A.5 SECTION A-A (FIGURE A.4) SHOWING ANNULAR REGIONS USED IN DERIVATION OF FUEL 1, FUEL 2, D_2O1 ETC. CROSS SECTIONS